Biophysical Journal Volume 67 August 1994 782–792

Passive and Active Tension in Single Cardiac Myofibrils

Wolfgang A. Linke, Victor I. Popov, and Gerald H. Pollack
Center for Bioengineering, University of Washington, Seattle, Washington 98195 USA

ABSTRACT Single myofibrils were isolated from chemically skinned rabbit heart and mounted in an apparatus described previously (Fearn et al., 1993; Linke et al., 1993). We measured the passive length-tension relation and active isometric force, both normalized to cross sectional area. Myofibrillar cross sectional area was calculated based on measurements of myofibril diameter from both phase-contrast images and electron micrographs. Passive tension values up to sarcomere lengths of approximately 2.2 μm were similar to those reported in larger cardiac muscle specimens. Thus, the element responsible for most, if not all, passive force of cardiac muscle at physiological sarcomere lengths appears to reside within the myofibrils. Above 2.2 μm, passive tension continued to rise, but not as steeply as reported in multicellular preparations. Apparently, structures other than the myofibrils become increasingly important in determining the magnitude of passive tension at these stretched lengths. Knowing the myofibrillar component of passive tension allowed us to infer the stress-strain relation of titin, the polypeptide thought to support passive force in the sarcomere. The elastic modulus of titin is 3.5×10^6 dyn cm^{-2}, a value similar to that reported for elastin. Maximum active isometric tension in the single myofibril at sarcomere lengths of 2.1–2.3 μm was 145 ± 35 mN/mm^2 (mean ± SD; $n = 15$). This value is comparable with that measured in fixed-end contractions of larger cardiac specimens, when the amount of nonmyofibrillar space in those preparations is considered. However, it is about 4 times lower than the maximum active tension previously measured in single skeletal myofibrils under similar conditions (Bartoo et al., 1993).

INTRODUCTION

Until now, passive and active properties of cardiac muscle have been measured largely by employing multicellular preparations, such as papillary muscles and trabeculae (Sonnenblick, 1967; Krueger and Pollack, 1975; ter Keurs et al., 1980; Kentish et al., 1986). Some investigators, almost two decades ago, advanced the state of the art by introducing the single isolated cell preparation (Fabiato and Fabiato, 1976; Tarr et al., 1979; Krueger et al., 1980), which allowed measurements to be made on a finer scale. Nevertheless, many basic issues of cardiac mechanics remain unresolved (Brady, 1991a).

Single myofibrils, when used for mechanical experiments, hold several advantages over larger preparations. Because measured tension is borne by the very sarcomeres in view, there is little room for ambiguity of interpretation (Bartoo et al., 1993). Also, with a myofibril approximately 1 μm in diameter, diffusion coefficients (e.g., 10^{-5} to 10^{-7} cm^2 s^{-1} for Ca^{2+}; Kushmerick and Podolsky, 1969) are high enough that the ion distribution is expected to remain nearly uniform (Cooke and Pate, 1985); thus, activation should be essentially uniform. Altogether, interpretation of data from single myofibril experiments appears to be particularly clear.

In this study, we employed single cardiac myofibrils to measure the passive length-tension relation and the maximum active isometric tension level. Although during the past years, several reports have appeared on force measurements using isolated myofibrils (Iwazumi, 1987; Okamura and Ishiwata, 1988; Bartoo et al., 1993; Friedman and Goldman, 1993), the present study is, to our knowledge, the first one that for mechanical experiments uses myofibrils from mammalian heart. Results obtained with single cardiac myofibrils, although largely comparable with those reported in multicellular cardiac preparations, allow one to characterize unambiguously passive and active properties at a level close to molecular, without the need to sacrifice the integrity of the filament lattice.

MATERIALS AND METHODS

Myofibril isolation

Isolated myofibrils were prepared from right ventricular wall tissue as described previously (Linke et al., 1993). Occasionally, we also used atrial tissue or papillary muscles. Briefly, thin strips of muscle tissue were dissected for storage in rigor/glycerol (50/50 by volume) solution for a minimum of 5 days at −20°C. To obtain single myofibrils, the glycerinated strips were minced, and the pieces were further skinned in 4°C rigor solution containing 0.5% Triton X-100 for 0.5–1 h. After washing with fresh rigor solution, the tissue pieces were homogenized in a blender (Sorvall Omni Mixer) at low speed for 5–6 s in the same buffer. A drop of this suspension was placed in the specimen chamber (volume, approximately 300 μl), and myofibrils were allowed to settle. From myofibrils that adhered lightly to the chamber bottom, one specimen was picked up by two microneedles tip-coated with a silicone adhesive (3145 RTV, Dow Corning; Fig. 1). Although we used mostly single myofibrils, we sometimes selected doublets.

Solutions

All experiments were performed at room temperature (20–22°C). Solutions were prepared according to a computer program (Coby, 1987) for the calculation of component concentrations based on solution algorithms developed by Fabiato and Fabiato (1979). Relaxing and activating solutions had a total ionic strength of 200 mM (adjusted with KOH) in a MOPS buffer, pH 7.1, and contained 3 mM magnesium methanesulfonate, 5 mM dipotassium methanesulfonate, 4 mM Na_2ATP, 0.05 mM leupeptin, and 15 mM

Received for publication 22 February 1994 and in final form 25 May 1994.

Address reprint requests to Wolfgang A. Linke, Center for Bioengineering, University of Washington, WD-12, Seattle, WA 98195. Tel.: 206-685-2744; Fax: 206-685-3300; E-mail: linke@bioeng.washington.edu.

0006-3495/94/08/782/11 $2.00

EGTA. In activating solutions, appropriate amounts of calcium methanesulfonate were added to obtain calcium concentrations of 10^{-7} M (pCa 7.0), 10^{-6} M (pCa 6.0), $10^{-5.5}$ M (pCa 5.5), 10^{-5} M (pCa 5.0), and $10^{-4.5}$ M (pCa 4.5), respectively.

Force transducer and experimental setup

Both experimental apparatus (Bartoo et al., 1993; Linke et al., 1993) and force transducer (Fearn et al., 1993) have been described in detail. Briefly, the two glass needles holding the myofibril are attached to a piezoelectric motor and a force transducer, respectively. Both devices are mounted on hydraulically controlled micromanipulators (Narishige, Model 102, Tokyo, Japan). The force transducer operates on the basis of a stiff, displaceable optical fiber (beam diameter, 70 μm) that at its distal end emits a cone of light illuminating a pair of receiving optical fibers. When force is exerted on the emitting fiber by an attached myofibril, the beam is deflected according to the amount of force applied. The force transducer's resonant frequency is typically 500 Hz, compliance 16 nm/μg force, and resolution better than 1 μg (10 nN).

The experimental setup is centered around a Zeiss Axiovert 35 inverted microscope equipped with phase-contrast optics, and placed on an air suspension table. The myofibril image can be projected onto either a high resolution CCD video camera (Sony XC-77RR), or a 512-element linear photodiode array (Reticon Electronics, model RL0512K). Collection of tension and sarcomere length data is done with a Macintosh II computer and MacAdios analog/digital interface. Software is written in C language.

Measurement of myofibril dimensions

Sarcomere length (SL) was measured by employing two alternative techniques. One, utilizing video images recorded by the CCD camera and image-processing software (National Institutes of Health Image Program, public domain software), measured the distance between the Z lines of consecutive sarcomeres. The other, using data collected by the photodiode array, measured the distance between the centers of mass of A bands or I bands (Linke et al., 1993), with a maximum error of approximately $\pm$50 nm per sarcomere (the larger the number of sarcomeres included in the measurement, the smaller the error). Both techniques gave similar results.

Myofibril width was recorded at slack SL in relaxing solution. It was measured by analyzing the intensity profile perpendicular to the myofibril axis, in the myofibril's center. Image-processing software was the same as that mentioned above. From the profile plot, pixel positions at half-maximum peak height were taken to define the two edges of the myofibril. To test whether width was uniform, the myofibril was rotated by 90 degrees around its length axis, and the measurement was repeated. Because it was not possible to rotate the preparation with the force transducer in place, the myofibril (at the end of each experiment) was loosened from the transducer needle with the help of a third needle, and the transducer was replaced by a simple needle holder.

Cross sectional area was calculated by assuming either a circular shape or, if more appropriate, an elliptical shape (by using major and minor width values).

In the phase-contrast images, the small dimensions of the myofibril preparation could potentially result in mis-estimation of width values. For example, in a single myofibril typically 1 μm (7 pixels) wide, resolution limitations prevented precise localization of the specimen edges (error, approximately $\pm$0.2 μm). To check for such possible mis-estimation, width values in the phase-contrast images were compared with those measured by electron microscopy. For this, cross sections of fixed and embedded specimens were prepared, and the average myofibril diameter was measured directly from the micrographs (see below).

Electron microscopy

Electron micrographs were prepared from intact muscle, myofibril suspensions, and single myofibrils, i.e., at three different stages in the process of myofibril isolation. The former two preparations were used to obtain cross sectional images of myofibrils. The preparation procedure was as follows: specimens were fixed in relaxing solution containing 2.5% glutaraldehyde, and the suspension was centrifuged to obtain a pellet of myofibrils. Both preparations were postfixed with osmium tetroxide in sodium cacodylate buffer, passed through a graded ethanol series for dehydration, and washed in 100% acetone. The specimens were then embedded in Epon 812/Araldite M, and thin cross sections were examined in an electron microscope (80 kV, model EM-1200 EX II, JEOL).

In addition, selected single myofibrils were recovered for EM observation after these specimens had been used for mechanical experiments. Preparation was done by lowering the entire assembly of myofibril and needle holders onto the surface of a glass slide coated with silicone (Sigmacote, Sigma Chemical Co., St. Louis, MO). The myofibril was glued (3145 RTV, Dow Corning) at either end onto the coverglass with the help of a third needle, fixed by adding 1% glutaraldehyde to the relaxing solution, and later postfixed with 1% osmium tetroxide. The specimen (on the cover glass) was then dehydrated by passage through a graded ethanol series and embedded in Epon 812/Araldite M by placing a resin-filled capsule on top of the cover glass, so that the myofibril was positioned in the approximate center of the capsule's opening. Knowing the myofibril's position facilitated sectioning and preparation for EM observation. Longitudinal sections were cut and examined in the electron microscope.

Stretch protocol

Myofibrils were held at slack length in relaxing solution and stretched to a selected length. Stretch duration was 6.24 s. After the specimens had been held at the new length for 90 s, they were released again to their slack length. During this stretch protocol, tension was recorded every 624 ms. The tension value at the end of the stretch period (after stress relaxation) was used for plotting the length-passive tension curve.

In some experiments, the active-force suppressing drug 2,3-butanedione monoxime (BDM) at concentrations of 10–100 mM (West and Stephenson, 1989) was applied to the relaxing solution, and passive tension was measured as described above.

Active tension measurement

Tension data during activation were collected at intervals of 624 ms. By performing activation at room temperature, it was ensured that the temperature of added solutions was similar to that of current bathing solutions and thus, temperature-induced variations of the force transducer response were minimized.

Before each activation, fresh relaxing solution was infused into the specimen chamber and SL was set between 2.1 and 2.3 μm. Initially, myofibrils were activated with intermediate calcium concentrations (pCa 6.0–5.5) and relaxed again, before full-activation solution (pCa 5.0–4.5) was applied. Activation was facilitated by slowly injecting activating solution into the sample chamber through a syringe, while simultaneously removing solution on the other side of the chamber by a second syringe. Care was taken to keep the solution volume within the chamber constant. After typically 1 min of activation, relaxation was induced by either adding a few tens of microliters of EGTA (200 mM) to the solution or by exchanging activating solution for relaxing solution. Finally, baseline tension values before and after activation were compared.

RESULTS

Specimen quality

Because single isolated myofibrils from mammalian cardiac muscle had not yet been investigated before this study, particular attention was paid to the quality of the specimen. One of several important factors is structural preservation. When viewed by phase-contrast microscopy, myofibrils exhibited good contrast between I and A bands (Fig. 1). To better judge

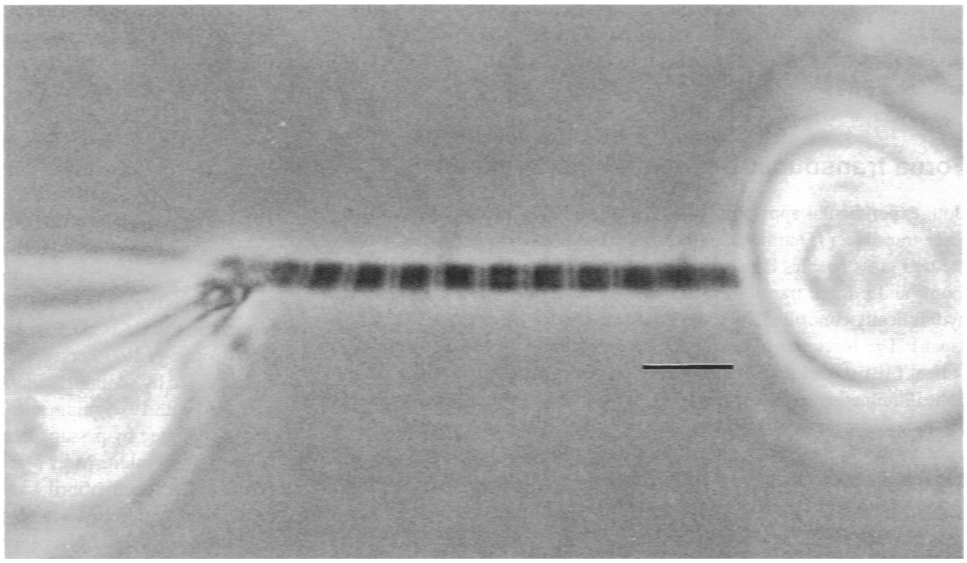

FIGURE 1 Phase-contrast image (100× objective) of an 11-sarcomere-long myofibril, stretched in relaxing solution to an SL of approximately 2.4 μm. The specimen was glued to two fine glass needles, one connected to a motor (*left*), the other to a force transducer (*right*). From the left needle tip, most glue was removed to enhance resolution near the myofibril end. Scale bar = 5 μm.

preservation at the ultrastructural level, specimens were examined by EM. Fig. 2 shows a longitudinal section of part of a relaxed myofibril. This same myofibril had been activated once and used for passive tension measurements. Thick and thin filaments, as well as M-lines and Z-lines, appear well organized. Sarcoplasmic reticulum is completely absent. As far as we can tell, all visible structures are not noticeably different from those seen in typical pictures of intact-muscle myofibrils in the literature. Thus, the single myofibrils appear morphologically intact.

Another important issue concerns the effect of myofibril isolation procedure. For example, overstretch of myofibrils in rigor solution during the preparation process may damage contractile proteins, which could result in reduced maximum active tension levels (Iwazumi, 1987). Therefore, we selected only myofibrils whose SL in rigor differed from their slack SL in the relaxed state by less than 5%. Resting, slack SL was 1.93 ± 0.13 μm (mean ± SD; n = 22 myofibrils) and, thus, was similar to data from the literature (Fabiato and Fabiato, 1976; De Clerck et al., 1984; Kentish et al., 1986; Brady, 1991a). A slight but statistically insignificant (p > 0.05, Student's t-test), difference was found between relaxed myofibrils before and after calcium activation (1.97 ± 0.14 vs. 1.90 ± 0.10 μm; n = 22 and 13, respectively). Altogether, myofibrils selected carefully with respect to their SL appeared to produce maximum tension values comparable with those reported in larger cardiac preparations (cf. Active Tension below).

During activation, myofibrils exhibited some deterioration. Both the contrast in the striation pattern and SL

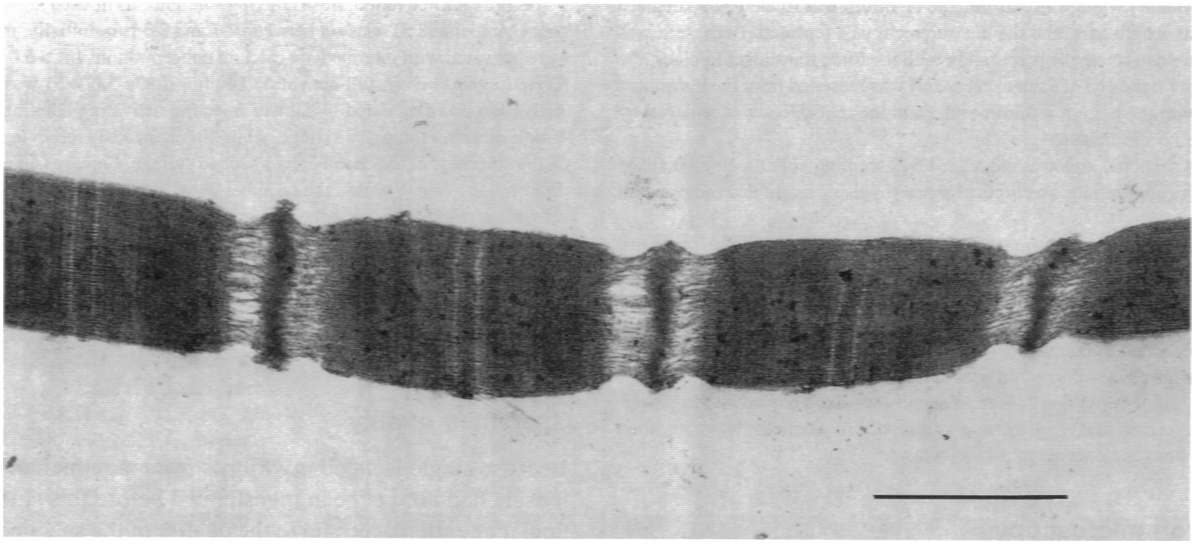

FIGURE 2 Electron micrograph of part of a single myofibril prepared after mechanical measurements. Ultrastructure is well preserved. Sarcoplasmic reticulum is absent. The myofibril was fixed in relaxing solution, and longitudinal sections were prepared as described in the *Methods* section. Resting SL is 2.0 μm. Scale bar = 1 μm.

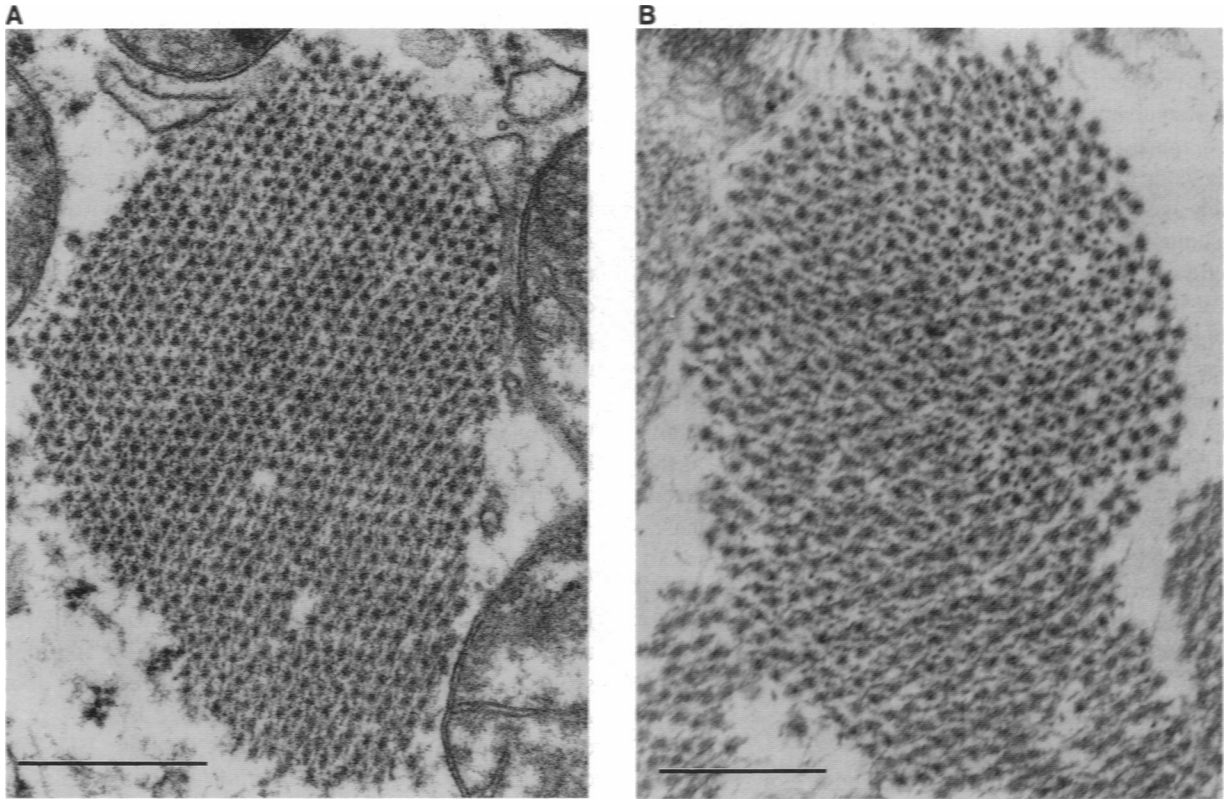

FIGURE 3 Electron micrographs of cross sectioned myofibrils fixed in relaxing solution. (*A*) myofibril from intact papillary muscle cell. Scale bar = 0.4 μm; (*B*) myofibril from suspension, after skinning and homogenization of ventricular tissue. Scale bar = 0.3 μm.

homogeneity decreased, but returned to nearly pre-activation levels after relaxation (cf. Active Force below). Brief ramp releases and re-stretches between activations (Brenner, 1983) did not appear to diminish SL inhomogeneity. During the first two to four activation cycles, maximum tension levels remained relatively stable and reproducible, but generally declined with further activations. Thus, performance of cardiac myofibrils declined after fewer contractions than that of single skeletal myofibrils, which could usually be activated 4 to 8 (sometimes more than 10) times before deterioration began (Bartoo et al., 1993). In short, the types of deterioration observed in isolated cardiac myofibrils are comparable with those seen in larger skinned cardiac preparations (Kentish et al., 1986; Sweitzer and Moss, 1993).

Myofibril width and cross sectional area

Myofibril width, measured from video images, was 1.13 ± 0.20 μm (mean ± SD; n = 47). This value is an average computed from measurements of both major and minor widths (cf. Materials and Methods). The relatively high SD (18%) resulted not only from differences between width values of a given myofibril, but also from variability among specimens.

Electron micrographs of cross sectioned specimens, both intact and skinned, also revealed considerable diversity of myofibril shape and diameter. Examples are shown in Fig. 3, *A* and *B*. Because most of the specimens exhibited more-or-less elliptical, rather than circular shape, we generally measured both major and minor myofibril diameters. Table 1 summarizes the results of diameter measurements. In intact, as well as in skinned preparations, average diameter was approximately 0.9 μm, with SDs of about ±40%.

To determine the amount of shrinkage resulting from EM preparation procedures, we measured the average lateral spacing of thick filaments from electron micrographs, and compared it with that reported in x-ray diffraction studies (Table 1). In intact cardiac muscle, we found an average

TABLE 1 EM measurements of myofibril cross section

	Intact muscle		Myofibril suspension	
	Measured	Corrected (according to x-ray data)	Measured	Corrected (according to x-ray data)
Thick filament spacing (nm) (mean ± SD)	40.5 ± 5.4 (n = 132)	42.6 ± 5.7 (n = 132)	44.5 ± 7.1 (n = 62)	46.2 ± 7.4 (n = 62)
Myofibril diameter (μm) (mean ± SD)	0.89 ± 0.36 (n = 132)	0.94 ± 0.38 (n = 132)	0.90 ± 0.39 (n = 62)	0.93 ± 0.40 (n = 62)

interfilament spacing of 40.5 nm; this value is about 5% smaller than the average value typically reported in x-ray studies for relaxed intact cardiac muscle at SLs slightly above 2 μm (Matsubara, 1980; Matsubara and Millman, 1974). In skinned muscle, we measured an average thick filament spacing value of 44.5 nm, which is approximately 4% smaller than the average value for skinned muscle obtained from x-ray studies (Matsubara, 1980). Thus, the EM preparation-induced lateral shrinkage was relatively small in magnitude and consistent in both intact and skinned specimens. The shrinkage values were used to correct the measured myofibril-diameter values (Table 1).

Because the EM method is more reliable than the optical technique in measuring micron-scale dimensions (after suitable shrinkage correction), we adopted the EM method as the "gold standard" for diameter measurements. Diameters measured by EM differed from those measured by phase-contrast microscopy, by approximately 20%. Therefore, all optical measurements of diameter were scaled down by 20%. These adjusted values were assumed closer to the actual dimensions and were used for all further calculations.

Passive tension

Tension tracings obtained in a representative experiment are shown in Fig. 4. The single myofibril was stretched from its slack length of 1.85 μm to each of six different SLs. A measurable stress appeared slightly above 2.0 μm. In this, as well as in most other experiments, slack SL after release was not different from that before stretches up to approximately 3.0 μm. Only when the myofibril was stretched to SLs beyond 3.0 μm and released again was slack length increased irreversibly. This increase became particularly evident after sarcomere stretch to lengths of 3.5 μm and above. Remarkably, however, even with those extreme stretches, SLs remained very homogeneous (average SL variation at 4.0 μm: ±5.2%; n = 7 myofibrils; 76 sarcomeres).

The amount of stress relaxation was variable. In the experiment of Fig. 4, stress relaxation was detectable at SLs above 2.5 μm and became more and more evident with larger stretches. In other experiments, it could sometimes be observed at SLs well below 2.5 μm. Generally, the magnitude of stress relaxation became noticeably larger when the speed of stretch was increased by more than 10 times (data not shown).

A summary of results of all stretch experiments is shown in Fig. 5. Passive tension increased steadily with SL (*lower solid curve*). This increase was not exponential, as it is in multicellular preparations (cf. *dotted*, *dashed/dotted*, and *dashed curve*); rather, the data could be well fitted with a polynomial equation. Although not shown in Fig. 5, we usually observed a strain limit (or "yield point"; Wang et al., 1991, 1993) at SLs between 3.2 and 3.5 μm. At such lengths, tension increase was less steep and, sometimes, the curve became flat. Tension values at the strain limit ranged between 110 and 150 mN/mm^2.

Effect of BDM on passive tension

BDM in millimolar concentrations is known to suppress active force in a dose-dependent manner (West and Stephenson, 1989). For example, at concentrations equal or above 50 mM, active force production is reduced by 90% or more, compared with the control value. By applying BDM in concentrations of 10, 50, and 100 mM to relaxing solution, we investigated whether residual interactions between thick and thin filaments, i.e., residual force-generating cross-bridges, contribute to passive tension. As shown in Fig. 5, no effect could be detected at any concentration. Therefore, residual interactions do not appear to underlie passive force.

Active force

Partial calcium activation

At intermediate activation levels (pCa 6.0–5.5), we generally observed SL oscillations. They usually originated at one end of a myofibril and propagated along the specimen in a wave-like manner. Characteristically, the oscillations consisted of repeated cycles of slow shortening and rapid lengthening.

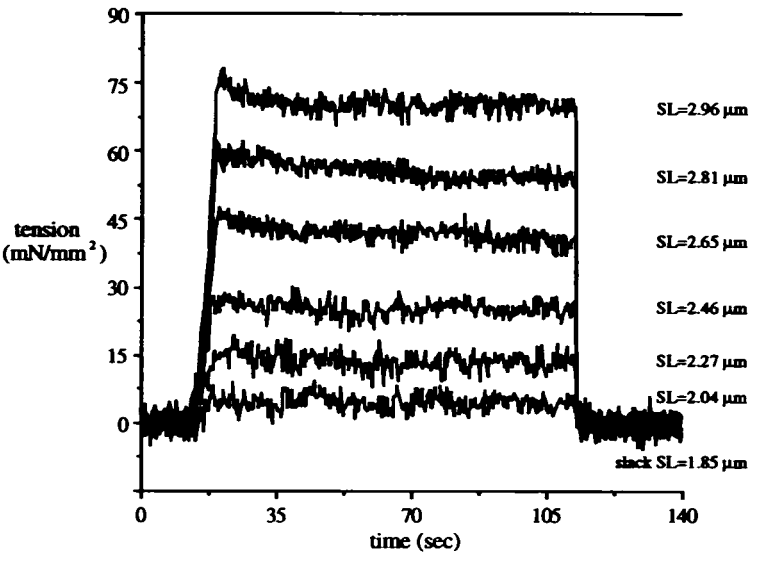

FIGURE 4 Passive tension tracings for stretches of a relaxed myofibril (25 sarcomeres long) to each of six different SLs. Stress relaxation was not noticeable until stretch exceeded an SL of approximately 2.5 μm. After stress relaxation, tension levels remained stable until the myofibril was released to slack length. SL after release was not different from that before stretch, except when stretched SL exceeded about 3 μm.

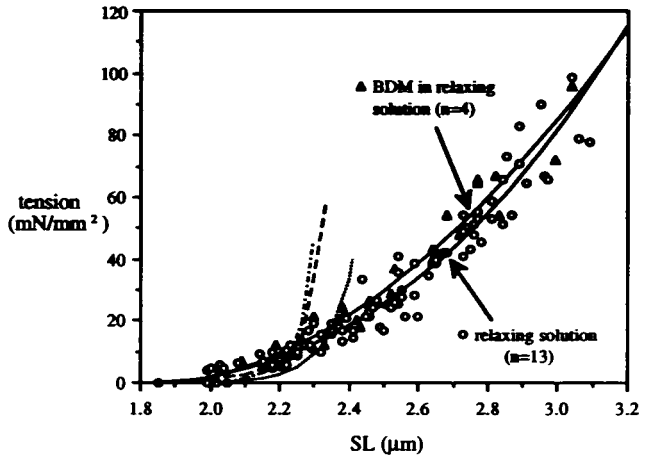

FIGURE 5 Length-passive tension relation in single cardiac myofibrils (——). Lower curve (corresponding to ○): polynomial curve fit for data from myofibrils in relaxing solution. Upper curve (corresponding to ▲): polynomial curve fit for data from myofibrils in relaxing solution containing BDM at concentrations of 10, 50, and 100 mM (the 50 mM concentration was tested on two myofibrils, each of the other concentrations on one myofibril). A strain limit, although not shown in the figure, was usually found at SLs between 3.2 and 3.5 μm. The dashed, dashed/dotted, and dotted lines correspond to passive tension data from intact rabbit papillary muscle (Julian et al., 1976), intact rat trabeculae, and skinned rat trabeculae (Kentish et al., 1986), respectively.

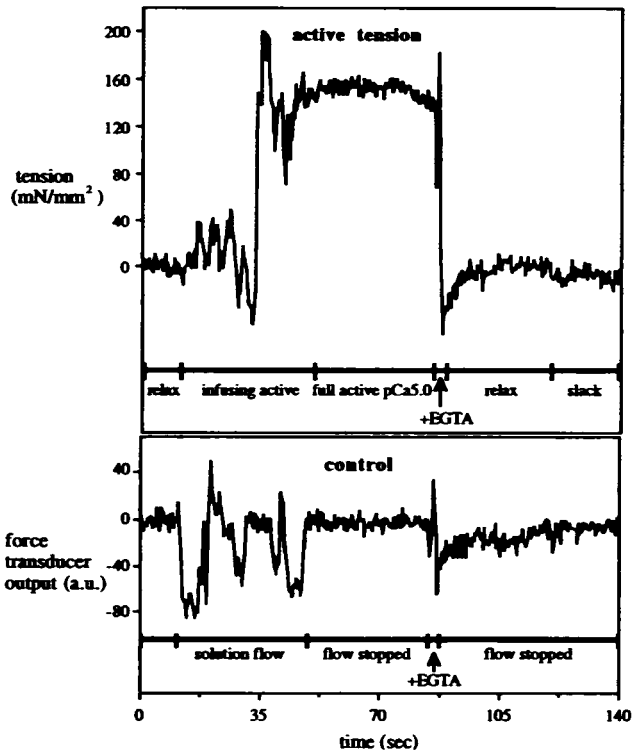

FIGURE 6 (*top*) Active tension tracing for pCa 5.0. This was the second full activation of an experimental series. The myofibril was 18 sarcomeres long and had a width of approximately 1.1 μm. SL before activation was 2.1 μm. Baseline tension was equal before and after activation. The activation protocol is indicated below the force tracing. (*bottom*) Force transducer response (no myofibril mounted) to perturbations within the specimen chamber, induced either by solution flow, or by application of 30 μl EGTA (200 mM). The unit (a.u. = arbitrary units) was chosen to have the same dimension as the unit (mN/mm²) in the top trace.

Sometimes, we could detect accompanying force oscillations whose magnitude was always less than 5% of maximum force at full activation. If not terminated by addition of either EGTA, relaxing, or fully activating solution, the oscillations could last tens of minutes, or even one hour. In a previous study, we characterized such oscillations in detail (Linke et al., 1993). The oscillations are not related to sarcoplasmic reticulum-Ca^{2+} release and uptake, for the myofibril preparation lacks functional SR. The phenomenon is potentially explainable on the basis of a strong length dependence of myofibrillar Ca^{2+} sensitivity.

Full calcium activation

A representative force tracing is shown in Fig. 6 (*top*). This tracing was obtained from a third activation, after the myofibril had previously been activated at pCa 6.0 (tension, 50 mN/mm²) and 5.0 (tension, 140 mN/mm²), respectively. Active tension at pCa 5.0 reached approximately 150 mN/mm² and exhibited a relatively steady activation plateau. After addition of EGTA, tension dropped back to zero. The transient dip below zero was confirmed to be an artifactual effect of EGTA on the force transducer (cf. Fig. 6, *bottom*). At the end of the protocol, the myofibril was released to below slack length to test whether relaxation was complete. Indeed, the small tension drop observed was no larger than expected from the passive stress level at an SL of 2.1 μm. Finally, in a fourth activation of that experimental series, the myofibril still developed a maximum force of 120 mN/mm² (pCa 4.5).

Fig. 7 shows a series of video images obtained before, during, and after activation in another myofibril. (Note lower fidelity of video images relative to photographic images such as that of Fig. 1.) In the upper image, the relaxed myofibril had an SL of 2.28 ± 0.10 μm (mean ± SD; n = 10 sarcomeres). Frames 2 and 3 show the myofibril partially activated. We observed SL oscillations of the type described above (cf. Partial Calcium Activation). Images 4 and 5 were obtained from the fully activated myofibril, which developed a force of 135 mN/mm². The images were taken 20 s apart. No sarcomeric motion is detectable. Relative to the relaxed myofibril, SL inhomogeneity was increased (SD, ±0.31 μm; n = 10). In the middle third of the myofibril, sarcomeres shortened (SL, 1.86 ± 0.08 μm; n = 4) at the expense of the end sarcomeres. The outermost right sarcomere, for example, exhibited an SL of 2.50 μm. We noted a small decrease in average SL, compared with the relaxed specimen (2.19 vs. 2.28 μm). This decrease was partly due to the deflection of the force transducer needle (Fig. 7, *right*), and partly to stretch of the left-end sarcomere, which had not been included in the SL measurement, because resolution was degraded by proximity to the needle. Finally, image 6 shows the same myofibril after activation. Sarcomere length averaged 2.27 ± 0.13 μm (n = 10) and, thus, SL values had returned to pre-activation levels.

To characterize SL homogeneity quantitatively, we computed the SDs of SL measurements along each myofibril.

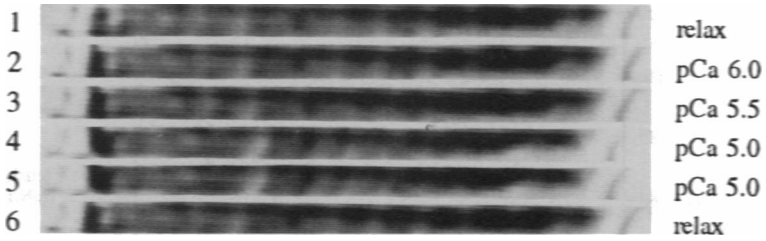

FIGURE 7 Series of video images before, during, and after activation of a myofibril. Visible at both ends of the myofibril are a part of the motor needle (*left*) and the force transducer needle (*right*). Resolution is relatively low in these video images, compared with the photograph of a myofibril (cf. Fig. 1). For further details, see text.

Table 2 shows the results. SLs remained very homogeneous, both before and after partial activation. Full activation tripled SL inhomogeneity. On the other hand, when attention was restricted to the more shortened central sarcomeres (average shortening, about 15%), the SD was much smaller. Thus, central sarcomeres were dynamically homogeneous. Relaxation of fully activated specimens reduced the degree of SL inhomogeneity to values slightly higher than, but not significantly different from those before activation ($p > 0.05$, Student's t-test).

It is noteworthy that myofibrils actively shortened under no load to SLs of 1.6 μm, or even below (for instance, specimens on the chamber bottom), did not re-lengthen spontaneously when exposed to relaxing solution. However, when those myofibrils were stretched in relaxing solution, they regained their original slack SL. This finding implies that the elements responsible for the restoring forces after unloaded shortening in larger cardiac specimens, even cells, are located outside the myofibril.

Single cardiac myofibrils typically developed 80–100 nN of maximum active force (pCa 5.0–4.5). Force per unit cross sectional area averaged 145 ± 35 mN/mm^2 (mean ± SD; n = 15). A force-pCa curve was calculated from the data of six experiments, using the Hill equation (Fig. 8). Maximum force was usually reached at pCa 5.0. The major parameters of the Hill equation, i.e., pCa_{50} and Hill coefficient (5.55 and 1.92, respectively), were similar to literature data from larger skinned cardiac preparations under comparable pH and ionic strength conditions (average pCa_{50}: 5.61; average Hill coefficient: 2.09; Fabiato, 1981; Kentish, 1984; Hofmann et al., 1991; Sweitzer and Moss, 1993).

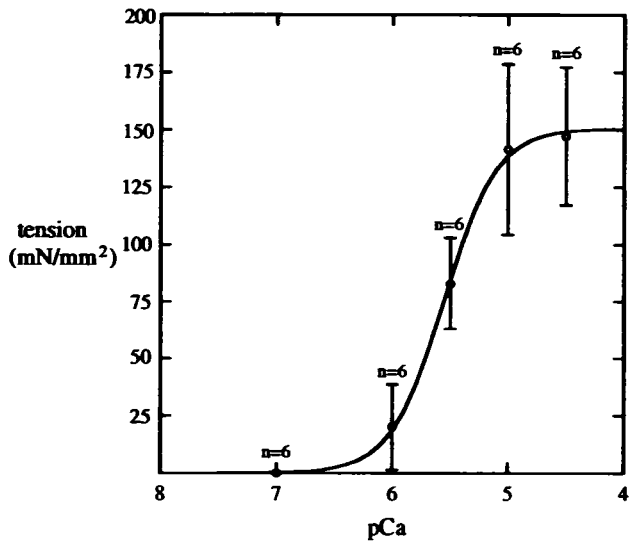

FIGURE 8 Tension-pCa curve for isolated cardiac myofibrils. Each data point represents an average of six measurements from six myofibrils (error bars = SD). Curve fit was done using the Hill equation.

DISCUSSION

Passive tension

A major issue in cardiac-muscle mechanics is the origin of passive tension (Brady, 1991a). In early reports, myocardial passive tension had been ascribed to stiff extracellular structures, such as collagen (e.g., Brady, 1968). With the arrival of the single cell preparation, however, it became clear that passive tension resides at least partly in the myocyte itself (e.g., Fabiato and Fabiato, 1978). But it has been difficult to ascertain the specific sub-cellular structures responsible for this tension since all preparations used to date contain diverse parallel elements, any of which could support passive force.

By using single myofibrils, we were able to measure the passive tension arising exclusively from structures within the sarcomere. We found that the myofibril/or sarcomere exhibited substantial resting tension. This tension was detectable at an SL around 2 μm and increased monotonically with stretch (Fig. 5). More interesting, perhaps, is the issue of how this passive length-tension relation compares with that measured in larger cardiac preparations, for such comparison can reveal the fraction of myocardial resting tension borne by the myofibril and the fraction borne by structures outside the myofibril.

TABLE 2 Standard deviations from SL measurements—indices of SL homogeneity

	SD (in %) (mean ± error)	No. sarcomeres	No. myofibrils
1st relaxing solution	3.9 ± 1.1	169	12
Intermediate Ca^{2+}	SL oscillations		
2nd relaxing solution	4.5 ± 1.2	281	18
Full Ca^{2+}, all sarcomeres	15.3 ± 3.8	137	8
Full Ca^{2+}, central sarcomeres	8.2 ± 3.4	47	8
3rd relaxing solution	7.2 ± 3.1	148	11

Comparison with larger cardiac specimens

In the larger cardiac specimens, nonmyofibrillar structures occupy a substantial volume fraction. To compare passive tension in such preparations with that measured here, it is necessary to compute the tension per myofibril. This requires

normalization for nonmyofibrillar space, which amounts to approximately 50% inside the cell (Sommer and Johnson, 1979), and 5–10% outside the cell (Weber et al., 1988). By multiplying force per unit area by a factor of 2–2.2, we therefore obtain tension per myofibril.

Applying this normalization factor, we find that over a major portion of the physiological SL range, 1.7–2.3 μm (Allen and Kentish, 1985), the magnitude of passive tension in larger cardiac preparations is similar to that in the single myofibril (cf. Fig. 5). Although in some earlier reports (e.g., Brady, 1968; Julian and Sollins, 1975), papillary muscle below 2.2 μm had been measured to have passive stress values two to 5 times higher than those of this study's myofibrils, more recent studies on intact cardiac specimens reported tension levels comparable with the values measured in single myofibrils (Krueger and Pollack, 1975; Julian et al., 1976; Kentish et al., 1986). In these earlier reports, resting, slack SLs were much shorter (1.5–1.6 μm) than those generally measured in more recent studies (average, around 1.9 μm; De Clerck et al., 1984; Kentish et al., 1986; Brady, 1991a), so that the older preparations might have been in partial contracture. In detergent-skinned cardiac myocytes, passive tension levels are also similar (Brady, 1991b). Any small differences (up to 25%) between these cells and the single myofibril in the physiological SL range are probably caused by experimental error and/or variations among species (Fabiato and Fabiato, 1978; Brady, 1991b). As far as we can tell, then, at least up to SLs of approximately 2.2 μm, single myofibrils and larger cardiac specimens exhibit comparable passive tension levels, implying that the source of passive stress lies mainly or exclusively within the myofibrils.

Beginning at SLs around 2.2 μm and above, passive tension in larger cardiac muscle preparations seems increasingly more determined by structures other than the myofibrils (cf. Fig. 5). These structures are likely to reside in the extracellular connective tissue rather than inside the cardiac cell (Brady, 1991a) and appear to be collagen. Such structures presumably help prevent the myocardium from overstretch (e.g., Borg et al., 1981; Robinson et al., 1988).

Ultrastructural basis of passive tension

In the single myofibril, passive tension could arise from at least two sources. One potential source is the contractile proteins, which even under relaxing conditions could still exhibit interactions. Of those interactions, weak-binding crossbridges can be discounted as contributors to passive tension (Granzier and Wang, 1993), which only leaves residual force-generating bridges as one possible source of passive tension. A second source is the connecting filament (sometimes referred to as the "titin" filament or the "connectin" filament; e.g., Trinick, 1991; Trombitas et al., 1993; Funatsu et al., 1993), which could support force elastically.

To test for the first possibility, we investigated the effect of the active-force-suppressing drug BDM on the shape of the passive length-tension curve (cf. Fig. 5). Because no effect was found, we felt we could exclude residual interaction between actin and myosin as a likely contribution to passive tension.

The connecting filament consists, at least in part, of the three-megadalton polypeptide known as titin (Wang, 1985; Trinick, 1991), which spans the entire distance between the M-line and Z-line. The A-band portion of titin is tightly bound to the thick filament along its entire length and, therefore, is functionally rigid, whereas the I-band portion is extensible (e.g., Trombitas et al., 1991; Wang et al., 1991). Thus, the connecting filament provides a functional elastic link between the end of the thick filament and the nearest Z-line. Therefore, it is in a unique position to support passive force in the sarcomere (Wang et al., 1993).

Knowing the passive tension in a single myofibril permits calculation of the force per single connecting filament. This calculation was made based on the following assumptions. First, a single myofibril averaging 0.93 μm in diameter consists of approximately 350 myosin filaments in parallel, as estimated from the results of EM measurements (cf. Table 1 above). Second, the myosin filament is flanked by a single connecting filament (Wang et al., 1993). Third, the connecting filament (in each half sarcomere) has zero extension at the measured slack SL of 1.93 μm (cf. Specimen Quality above; Funatsu et al., 1993). With these assumptions, we could infer the stretch-force relation of the single connecting filament. The shape of this relation is the same as that of the myofibrillar length-passive tension curve; only the magnitude is different. When the connecting filament is stretched by 0.1 μm, force is 12 pN; stretch by 0.3 or 0.5 μm results in forces of 60 and 150 pN, respectively.

From such calculations, we can also deduce the elastic behavior of a single titin strand, which is thought to represent the structural unit of the connecting filament (Wang, 1985; Maruyama, 1986; Trinick, 1991). The exact number of titin molecules per connecting filament is not certain, but most investigators have suggested that six titin strands exist in each half sarcomere (Maruyama, 1986; Whiting et al., 1989; Trinick, 1991). Using this number, we calculate the force necessary to stretch one cardiac titin molecule to be approximately 10, 20, and 28 pN, at SLs of 2.5, 2.8, and 3.0 μm, respectively. These are approximately 10 times the values similarly inferred in skinned frog skeletal muscle (Higuchi et al., 1993). Thus, at least at comparable sarcomere stretch, cardiac titin appears to be an order of magnitude stiffer than skeletal titin.

This line of approach also permits calculation of titin's elastic modulus. Such calculation is, of course, subject to error depending on the number of titin strands actually found in each connecting filament. (We base our calculation on an estimate of six titin molecules per connecting filament.) We assume a single-molecule diameter of 3.5 nm (Nave et al., 1989) and an approximate slack length of 0.15 μm for the extensible I-band portion of titin in each half sarcomere (as follows from resting SL, 1.93 μm; A-band length, 1.6 μm; I-band length, including Z-line width, 0.33 μm). Thus, titin would be stretched by 100%, at an SL of 2.23 μm. Then, by

assuming a linear stress-strain relation within the physiological SL range and expressing stress as force per titin cross sectional area, we calculate the elastic modulus of titin to be approximately 3.5×10^6 dyn cm^{-2}.

By contrast, the elastic modulus for chicken-skeletal-muscle titin was recently reported to be approximately 10^8 dyn cm^{-2} (Higuchi et al., 1993), which is almost two orders of magnitude higher than that estimated in this study. The reason for the difference is not clear, but might be related to the fact that skeletal titin stiffness was calculated from dynamic light-scattering measurements on isolated molecules, whereas in the present study, cardiac titin stiffness was estimated directly from mechanical measurements made on the intact sarcomere. Further studies are needed to reconcile these differences.

Mechanical characterization of titin is interesting with respect to the elastic properties of other biologically important elastic materials, such as collagen and elastin. For elastin, the elastic modulus has been reported to range from 2.6×10^6 dyn cm^{-2} (Urry, 1984) to 5×10^6 dyn cm^{-2} (Barra et al., 1993). Collagen has an elastic modulus almost three orders of magnitude higher than that of elastin (approximately 10^9 dyn/cm^{-2}; e.g., Barra et al., 1993). Thus, the modulus calculated for cardiac titin, 3.5×10^6 dyn cm^{-2}, is much smaller than that of collagen, but surprisingly similar to that of elastin.

Comparison with isolated skeletal myofibrils

In the single cardiac myofibrils studied here, passive tension became evident at shorter SLs than in isolated skeletal myofibrils (cf. Bartoo et al., 1993) and was considerably higher at all SLs. Comparable differences are known to exist in larger preparations (Fish et al., 1984).

From the results of passive tension measurements on single myofibrils from rabbit psoas muscle (Bartoo et al., 1993), we can deduce the elastic properties of a skeletal titin molecule in a manner similar to that described above for cardiac myofibrils. Assuming six titin strands per connecting filament (per half sarcomere), the force necessary to stretch one skeletal titin molecule (at SLs of 2.8, 3.0, and 3.5 μm, respectively) is approximately 0.8, 1.8, and 11 pN. These values, although much smaller than those inferred from cardiac myofibrils, are comparable with the values calculated by Higuchi et al. (1993) for skinned frog skeletal muscle (1.3, 2.6, and 7 pN, at respective SLs). Thus, titin molecules from skeletal and cardiac muscle may differ in their elastic properties.

Although variations in titin elasticity in the two muscle types (perhaps because of expression of different titin isoforms; cf. Wang et al., 1991) can explain differences in the passive length-tension relations, alternative possibilities should be considered. These include: (i) variations in the number of titin strands per connecting filament; (ii) differences in titin's slack length; and (iii) binding of cardiac-muscle titin to actin in the I-band (Funatsu et al., 1993), thereby increasing the resting stiffness of heart muscle relative to that of skeletal muscle.

Active tension

Comparison with larger cardiac preparations

Maximum isometric tension levels in intact papillary muscles and trabeculae, irrespective of species, usually range between 40 and 80 mN/mm^2 (Julian and Sollins, 1975; Huntsman et al., 1977; Dietrich and Elzinga, 1993; Hancock et al., 1993). Skinned preparations exhibit similar tension values (60–90 mN/mm^2; Kentish et al., 1986; Stienen et al., 1993). On the other hand, in situations in which internal sarcomere shortening is prevented (sarcomere-isometric contractions), active tension is usually higher. This increase has been reported to be approximately 50% (Donald et al., 1980), resulting in tension values above 100 mN/mm^2 (Krueger and Pollack, 1975; ter Keurs et al., 1980), although a value of only 50 mN/mm^2 was reported in one study (Julian et al., 1976).

The single myofibrils used in the present study developed tension values (average, 145 mN/mm^2) that are a priori higher than the values found in larger preparations. However, when the nonmyofibrillar space in a cardiac cell (approximately 50%; Sommer and Johnson, 1979) and the intercellular space (5–10% of tissue volume; Weber et al., 1988) are considered in larger preparations, force per unit cross sectional area under muscle-isometric conditions, is the same as in the single myofibril.

Sarcomere dynamics in the single myofibril were remarkably similar to those in larger specimens. We found internal sarcomere shortening of about 15% upon activation. Similarly, shortening of sarcomeres (up to 20%) during muscle-isometric contractions has normally been observed in the central region of larger cardiac specimens (Julian and Sollins, 1975; Krueger and Pollack, 1975; Huntsman et al., 1977, Kentish et al., 1986). In the myofibril preparation, internal sarcomere shortening (and stretch of the outer sarcomeres) perhaps results from mechanical damage of the specimen ends caused by the mounting procedure, as it has been demonstrated in larger preparations (Krueger and Pollack, 1975; Donald et al., 1980). Also, it cannot be excluded that some damaging effect on the end sarcomeres comes from the silicone glue, which releases trace amounts of methanol as it cures.

Comparison with skeletal myofibrils

Active isometric tension was recently measured in isolated skeletal myofibrils under conditions similar to the present study and was found to be approximately 600 mN/mm^2 (Bartoo et al., 1993). By comparison, the value measured here in cardiac myofibrils was 145 ± 35 mN/mm^2. Hence, skeletal myofibrils appear to generate considerably more force per cross sectional area than cardiac myofibrils.

Differences in active tension have generally been found between skeletal and cardiac muscle preparations. Intact and skinned skeletal muscles typically develop forces of 230–300 and 150–230 mN/mm^2, respectively (for references, cf. Bartoo et al., 1993), compared with only 40–90 mN/mm^2 in

intact or skinned cardiac muscle (cf. this section, above). These differences have been attributed mainly to variations in cellular myofibril content. However, because the fraction of myofibril volume in a skeletal muscle cell (83–92%; Eisenberg et al., 1974) is less than twice that in a cardiac muscle cell (50%; Sommer and Johnson, 1979), the differences in tension level cannot be explained by variations in cellular myofibril content alone.

This study's findings suggest that the difference in maximum force level between the two muscle types lies at least partly in different force-generating abilities of the contractile proteins. Variations in myosin heavy chain isoforms might play an important role. Specificity of heavy chain composition has already been shown to determine the amount of maximum force, at least in different types of skeletal muscle: tension differed by up to 100% in slow and fast fibers, respectively (Eddinger and Moss, 1987; Bottinelli et al., 1991), although such differences have not consistently been reported (Greaser et al., 1988). Furthermore, in a recent study employing isolated cardiac and skeletal myosins in an in vitro motility assay (where fluorescently labeled actin filaments move over a myosin-coated surface), Harris et al. (1994a and b) reported that in myosins from skeletal muscle, force per cross-bridge was up to 4 times higher than in myosins from cardiac muscle. This finding supports our conclusion that skeletal and cardiac myosins may differ in their maximum force-generating ability.

In summary, we present here the first detailed study of passive and active tension measurements in single isolated cardiac myofibrils. Two conclusions seem especially interesting. First, as best we can resolve, passive tension over most of the physiological SL range appears to reside in the connecting filament proteins, not in intermyofibrillar or extracellular structures. The connecting filament acts as a stiff spring, tending to restore the stretched sarcomere to its resting length. Second, and perhaps surprising, active tension levels in cardiac myofibrils are substantially lower than in skeletal myofibrils. Why cardiac muscle is thus "deficient" might arise out of a compromise between the ability to generate force and the need to contract an a continual, beat-by-beat basis.

We thank Dr. Karoly Trombitas, Marc Bartoo, and Eric Seibel for their helpful comments and suggestions. We are also grateful to John Myers, Jeff Magula, and Keith Johnson for their excellent technical assistance.

REFERENCES

Allen, D. G., and J. C. Kentish. 1985. The cellular basis of the length-tension relation in cardiac muscle. *J. Mol. Cell. Cardiol.* 17:821–840.

Barra, J. G., R. L. Armentano, J. Levenson, E. I. C. Fischer, R. H. Pichel, and A. Simon. 1993. Assessment of smooth muscle contribution to descending thoracic aortic elastic mechanics in conscious dogs. *Circ. Res.* 73:1040–1050.

Bartoo, M. L., V. I. Popov, L. A. Fearn, and G. H. Pollack. 1993. Active tension generation in isolated skeletal myofibrils. *J. Muscle Res. Cell Motil.* 14:498–510.

Borg, T. K., W. F. Ranson, F. A. Moslehy, and J. B. Caulfield. 1981. Structural basis of ventricular stiffness. *Lab. Invest.* 44:49–54.

Bottinelli, R., S. Schiaffino, and C. Reggiani. 1991. Force-velocity relations and myosin heavy chain isoform compositions of skinned fibres from rat skeletal muscle. *J. Physiol.* 437:655–672.

Brady, A. J. 1968. Active state in cardiac muscle. *Physiol. Rev.* 48:570–600.

Brady, A. J. 1991a. Mechanical properties of isolated cardiac myocytes. *Physiol. Rev.* 71:413–428.

Brady, A. J. 1991b. Length dependence of passive stiffness in single cardiac myocytes. *Am. J. Physiol.* 260:H1062;ENH1071.

Brenner, B. 1983. Technique for stabilizing the striation pattern in maximally calcium-activated skinned rabbit psoas fibers. *Biophys. J.* 41: 99–102.

Coby, R. 1987. Solution Mixing for Muscle Bathing Medium: A Handbook. University of Washington, Department of Physiology and Biophysics, Seattle, WA. 1–67.

Cooke, R., and E. Pate. 1985. The effects of ADP and phosphate on the contraction of muscle fibers. *Biophys. J.* 48:789–798.

De Clerck, N. M., V. A. Claes, and D. L. Brutsaert. 1984. Uniform sarcomere behaviour during twitch of intact single cardiac cells. *J. Mol. Cell. Cardiol.* 16:735–745.

Dietrich, D. L. L., and G. Elzinga. 1993. Heat produced by rabbit papillary muscle during anoxia and reoxygenation. *Circ. Res.* 73:1177–1187.

Donald, T. C., D. N. S. Reeves, R. C. Reeves, A. A. Walker, and L. L. Hefner. 1980. Effect of damaged ends in papillary muscle preparations. *Am. J. Physiol.* 238:H14;ENH23.

Eddinger, T. J., and R. L. Moss. 1987. Mechanical properties of skinned single fibers of identified types from rat diaphragm. *Am. J. Physiol.* 253: C210;ENC218.

Eisenberg, B. R., A. M. Kuda, and J. B. Peter. 1974. Stereological analysis of mammalian skeletal muscle. I. Soleus muscle of the adult guinea pig. *J. Cell Biol.* 60:732–754.

Fabiato, A. 1981. Myoplasmic free calcium concentration reached during the twitch of an intact isolated cardiac cell and during calcium-induced release of calcium from the sarcoplasmic reticulum of a skinned cardiac cell from the adult rat or rabbit ventricle. *J. Gen. Physiol.* 78:457–497.

Fabiato, A., and F. Fabiato. 1976. Dependence of calcium release, tension generation and restoring forces on sarcomere length in skinned cardiac cells. *Eur. J. Cardiol.* 4:13–27.

Fabiato, A., and F. Fabiato. 1978. Myofilament-generated tension oscillations during partial calcium activation and activation dependence of the sarcomere length-tension relation of skinned cardiac cells. *J. Gen. Physiol.* 72:667–699.

Fabiato, A., and F. Fabiato. 1979. Calculator programs for computing the composition of the solutions containing multiple metals and ligands used for experiments in skinned muscle cells. *J. Physiol.* 75:463–505.

Fearn, L. A., M. L. Bartoo, J. A. Myers, and G. H. Pollack. 1993. An optical fiber transducer for single myofibril force measurement. *IEEE Trans. Biomed. Eng.* 40:1127–1132.

Fish, D., J. Orenstein, and S. Bloom. 1984. Passive stiffness of isolated cardiac and skeletal myocytes in the hamster. *Circ. Res.* 54:267–276.

Friedman, A. L., and Y. E. Goldman. 1993. Force and force transients in bundles of 1–3 myofibrils from rabbit psoas muscle. *Biophys. J.* 64:345*a*. (Abstr.)

Funatsu, T., E. Kono, H. Higuchi, S. Kimura, S. Ishiwata, T. Yoshioka, K. Maruyama, and S. Tsukita. 1993. Elastic filaments in situ in cardiac muscle: deep-etch replica analysis in combination with selective removal of actin and myosin filaments. *J. Cell Biol.* 120:711–724.

Granzier, H. L. M., and K. Wang. 1993. Passive tension and stiffness of vertebrate skeletal and insect flight muscles: The contribution of weak cross-bridges and elastic filaments. *Biophys. J.* 65:2141–2159.

Greaser, M. L., R. L. Moss, and P. J. Reiser. 1988. Variations in contractile properties of rabbit single muscle fibres in relation to troponin T isoforms and myosin light chains. *J. Physiol.* 406:85–98.

Hancock, W. O., D. A. Martyn, and L. L. Huntsman. 1993. Ca^{2+} and segment length dependence of isometric force kinetics in intact ferret cardiac muscle. *Circ. Res.* 73:603–611.

Harris, D. E., S. S. Work, R. K. Wright, N. R. Alpert, and D. M. Warshaw. 1994a. Smooth, cardiac and skeletal muscle myosin force and motion generation assessed by cross-bridge mechanical interactions in vitro. *J. Muscle Res. Cell Motil.* 15:11–19.

Harris, D., N. Alpert, and D. Warshaw. 1994b. Smooth, skeletal and cardiac

muscle myosin force assessed by cross-bridge mechanical interactions in vitro. Presentation at the 38th Annual Meeting of the Biophysical Society, March 6–10, 1994, New Orleans, LA.

Higuchi, H., Y. Nakauchi, K. Maruyama, and S. Fujime. 1993. Characterization of β-connectin (titin 2) from striated muscle by dynamic light scattering. *Biophys. J.* 65:1906–1915.

Hofmann, P. A., H. C. Hartzell, and R. L. Moss. 1991. Alterations in Ca^{2+} sensitive tension due to partial extraction of C-protein from rat skinned cardiac myocytes and rabbit skeletal muscle fibers. *J. Gen. Physiol.* 97: 1141–1163.

Huntsman, L. L., S. R. Day, and D. K. Stewart. 1977. Nonuniform contraction in the isolated cat papillary muscle. *Am. J. Physiol.* 233: H613–H616.

Iwazumi, T. 1987. Mechanics of the myofibril. *In* Mechanics of the Circulation. H. E. D. J. ter Keurs and J. V. Tyberg, editors. Martinus Nijhoff Publishing, Dordrecht, The Netherlands. 37–49.

Julian, F. J., and M. R. Sollins. 1975. Sarcomere length-tension relations in living rat papillary muscle. *Circ. Res.* 37:299–308.

Julian, F. J., M. R. Sollins, and R. L. Moss. 1976. Absence of a plateau in length-tension relationship of rabbit papillary muscle when internal shortening is prevented. *Nature.* 260:340–342.

Kentish, J. C. 1984. The inhibitory effect of monovalent ions on force development in detergent-skinned ventricular muscle from guinea-pig. *J. Physiol.* 352:353–374.

Kentish, J. C., H. E. D. J. ter Keurs, L. Ricciardi, J. J. J. Bucx, and M. I. M. Noble. 1986. Comparison between the sarcomere length-force relations of intact and skinned trabeculae from rat right ventricle. *Circ. Res.* 58:755–768.

Krueger, J. W., and G. H. Pollack. 1975. Myocardial sarcomere dynamics during isometric contraction. *J. Physiol.* 251:627–643.

Krueger, J. W., D. Forletti, and B. A. Wittenberg. 1980. Uniform sarcomere shortening behavior in isolated cardiac muscle cells. *J. Gen. Physiol.* 76:587–607.

Kushmerick, M. J., and R. J. Podolsky. 1969. Ionic mobility in muscle cells. *Science.* 166:1297–1298.

Linke, W. A., M. L. Bartoo, and G. H. Pollack. 1993. Spontaneous sarcomeric oscillations at intermediate activation levels in single isolated cardiac myofibrils. *Circ. Res.* 73:724–734.

Maruyama, K. 1986. Connectin, an elastic protein of striated muscle. *Int. Rev. Cytol.* 104:81–114.

Matsubara, I. 1980. X-ray diffraction studies of the heart. *Annu. Rev. Biophys. Bioeng.* 9:81–105.

Matsubara, I., and B. M. Millman. 1974. X-ray diffraction patterns from mammalian heart muscle. *J. Mol. Biol.* 82:527–536.

Nave, R., D. O. Fürst, and K. Weber. 1989. Visualization of the polarity of isolated titin molecules: a single globular head on a long thin rod as the M band anchoring domain? *J. Cell Biol.* 109:2177–2187.

Okamura, N., and S. Ishiwata. 1988. Spontaneous oscillatory contraction of sarcomeres in skeletal myofibrils. *J. Muscle Res. Cell Motil.* 9:111–119.

Pollack, G. H., and J. W. Krueger. 1976. Sarcomere dynamics in intact cardiac muscle. *Eur. J. Cardiol.* 4:53–65.

Robinson, T. F., L. Cohen-Gould, S. M. Factor, M. Eghbali, and O. O. Blumenfeld. 1988. Structure and function of connective tissue in cardiac muscle: collagen types I and III in endomysial struts and pericellular fibers. *Scanning Microsc.* 2:1005–1015.

Sommer, J. R., and E. A. Johnson. 1979. Ultrastructure of cardiac muscle. *In* Handbook of Physiology. The Cardiovascular System, Sec. 2, Vol. 1. R. Burns, editor. American Physiological Society, Bethesda, MA. 113–186.

Sonnenblick, E. H. 1967. Series elasticity in heart muscle, its relation to contractile element velocity and proposed muscle models. *Circ. Res.* 20: 112–123.

Stienen, G. J. M., Z. Papp, and G. Elzinga. 1993. Calcium modulates the influence of length changes on the myofibrillar adenosine triphosphatase activity in rat skinned cardiac trabeculae. *Pflügers Arch.* 425:199–207.

Sweitzer, N. K., and R. L. Moss. 1993. Determinants of loaded shortening velocity in single cardiac myocytes permeabilized with α-hemolysin. *Circ. Res.* 73:1150–1162.

Tarr, M., J. W. Trank, P. Leiffer, and N. Shepherd. 1979. Sarcomere length-resting tension relation in single frog atrial cardiac cells. *Circ. Res.* 45: 554–559.

ter Keurs, H. E. D. J., W. H. Rijnsburger, R. van Heuningen, and M. J. Nagelsmit. 1980. Tension development and sarcomere length in rat cardiac trabeculae. *Circ. Res.* 46:703–714.

Trinick, J. 1991. Elastic filaments and giant proteins in muscle. *Curr. Opin. Cell Biol.* 3:112–118.

Trombitas, K., P. H. W. W. Baatsen, M. S. Z. Kellermayer, and G. H. Pollack. 1991. Nature and origin of gap filaments in striated muscle. *J. Cell Science.* 100:809–814.

Trombitas, K., G. H. Pollack, J. Wright, and K. Wang. 1993. Elastic properties of titin filaments demonstrated using a "freeze-break" technique. *Cell Motil. Cytoskel.* 24:274–283.

Urry, D. W. 1984. Protein elasticity based on conformations of sequential polypeptides: the biological elastic fiber. *J. Protein Chem.* 3:403–436.

Wang, K. 1985. Sarcomere-associated cytoskeletal lattices in striated muscle. Reviews and hypothesis. *In* Cell and Muscle Motility, Vol. 6. J. W. Shay, editor. Plenum Press, New York. 315–369.

Wang, K., R. McCarter, J. Wright, J. Beverly, and R. Ramirez-Mitchell. 1991. Regulation of skeletal muscle stiffness and elasticity by titin isoforms: a test of the segmental extension model of resting tension. *Proc. Natl. Acad. Sci. USA.* 88:7101–7105.

Wang, K., R. McCarter, J. Wright, J. Beverly, and R. Ramirez-Mitchell. 1993. Viscoelasticity of the sarcomere matrix of skeletal muscles. The titin-myosin composite filament is a dual-stage molecular spring. *Biophys. J.* 64:1161–1177.

Weber, K. T., J. S. Janicki, S. G. Shroff, R. Pick, R. M. Chen, and R. I. Bashey. 1988. Collagen remodeling of the pressure-overloaded, hypertrophied nonhuman primate myocardium. *Circ. Res.* 62:757–765.

West, J. M., and D. G. Stephenson. 1989. Contractile activation and the effects of 2:3-butanedione monoxime (BDM) in skinned cardiac preparations from normal and dystrophic mice (129/ReJ). *Pflügers Arch.* 413: 546–552.

Whiting, A., J. Wardale, and J. Trinick. 1989. Does titin regulate the length of thick filaments? *J. Mol. Biol.* 205:263–268.